*Russian Journal of General Chemistry, Vol. 73, No. 3, 2003, pp. 401–407. Translated from Zhurnal Obshchei Khimii, Vol. 73, No. 3, 2003, pp. 429–436.*


# Quantum-Chemical Study of Anisole Molecule

**V. M. Bzhezovskii and E. G. Kapustin**

*Institute of Organic Chemistry, National Academy of Sciences of Ukraine, Kiev, Ukraine*

Received August 11, 2000

**Abstract** — The potential functions of internal rotation around the $C_{sp^2}$–O bond in the $C_6H_5OCH_3$ molecule were obtained by HF/6-31G(*d*), MP2(f)/6-31G(*d*), and B3LYP/6-31(*d*) calculations. Hartree–Fock calculations reveal a fourfold barrier to internal rotation around the $C_{sp^2}$–O bond. The MP2 and B3LYP calculations reveal a twofold barrier with a height of 7.78 and 10.70 kJ mol$^{-1}$, respectively (corrected for the zero vibration energy). The molecular geometries, first Koopmans ionization potentials, and dipole moments are reported. Calculations for liquid anisole in the self-consistent reactive field (SCRF) continual model give the results that only slightly differ from the results obtained for the isolated molecule in a vacuum. Within the framework of the Natural Bond Orbitals formalism, the following parameters were determined: energy, degree of hybridization, and population of oxygen lone electron pairs and energy of their interaction with antibonding π* orbitals of the aromatic ring.

The most important conformational characteristic of anisole is the torsion (dihedral) angle φ between the planes of the benzene ring and $C_{sp^2}$–O–$C_{sp^3}$ bonds. In view of the molecular symmetry, the potential function of internal rotation of fragments about the $C_{sp^2}$ bond can contain any number of symmetrical ($0° \le \varphi \le 180°$ and $180° \le \varphi \le 360°$) energy minima. The extreme case of nonplanar conformation is the orthogonal form (φ 90° and 270°). The molecular conformation is governed by two major factors: *n*,π conjugation of the oxygen lone electron pairs with the π system of the aromatic ring, stabilizing the planar form, and the steric interactions of the *o*-hydrogen aroms of the ring with the hydrogen atom of the $CH_3$ group, preventing realization of the planar structure.

According to electron diffraction data [1, 2], the $C_6H_5OCH_3$ molecule in the gas phase at room temperature has a planar structure and hence a twofold rotation barrier. As the temperature is increased from 55 to 250°C, the planarity is distorted (φ 40°), and the rotation barrier becomes fourfold. The planar structure is confirmed by microwave [1, 3] and photoelectron [4, 5] spectroscopy. The Kerr effect method (birefringence in electric field) gives φ 22° [6] or 18° [7]. Analysis of long-range coupling constants in the NMR spectra, in combination with HF/6-31G and HF/6-31G(5*d*) calculations, led Schaefer and Sebastian [8] to a conclusion that internal rotation about the $C_{sp^2}$–O bond in anisole cannot be described assuming a twofold barrier. According to [8], the component of the twofold barrier is $15.0 \pm 2.0$ kJ mol$^{-1}$, and that of the fourfold barrier, $5.6 \pm 2.2$ kJ mol$^{-1}$. The rotation barrier measured for anisole in the gas phase by IR and Raman spectroscopy is 15.1 kJ mol$^{-1}$ [9]. Frige and Klessinger [10] evaluated the rotation barrier in the gas phase by photoelectron spectroscopy and obtained the value of 23.8 kJ mol$^{-1}$. Konshin and Tylli [11] revealed a strong temperature dependence of the 215 nm band in the UV spectra of gaseous anisole and attributed this fact to different absorption of several structures. The electronic absorption spectra and energies of the triplet state of anisole in planar and orthogonal conformations were calculated by the CNDO/S-CI method taking into account interaction of singly excited configurations [12]. The rotation barrier in liquid anisole, according to [13], is 25.1 kJ mol$^{-1}$. Tylli and Konschin [14] measured the Raman spectra of solid $C_6H_5OCH_3$ and $C_6H_5OCD_3$ at 130 K and estimated the rotation barrier at 50 kJ mol$^{-1}$. The fourfold rotation barrier about the O–$CH_3$ bond in solid anisole was estimated at 22.1 (planar conformation) and 20 kJ mol$^{-1}$ (orthogonal conformation) [15].

Quantum-chemical calculations with inclusion of correlation effect were performed in the MP2/6-31G(*d*) approximation for a limited set of fixed values of φ and other geometric parameters optimized on the HF/6-31G(*d*) level; this was followed by determination of the potential function of internal rotation by expansion of the torsion potential in Fourier series [16, 17]. The calculations reveal a twofold barrier to rotation about the $C_{sp^2}$–O bond with the energy minimum in the region of the planar conformation (φ 0°) and the transition state in the region of the orthogonal conformation (φ 90°). The rotation barrier is estimated

1070-3632/03/7303-0401 $25.00 

at ~9 to ~10 kJ mol$^{-1}$. Nicholas and Hay determined the energies of the minimum and transition state in the MP2/6-311+G(*d*) approximation and obtained the rotation barrier of 7.91 kJ mol$^{-1}$ [18]. Spellmeyer *et al.* [17] performed molecular-dynamic calculations for liquid anisole and estimated the rotation barrier at 6.3 kJ mol$^{-1}$.

The goals of this study are as follows: (1) comparative analysis of the potential functions of internal rotation around the $C_{sp^2}$–O bond in the anisole molecule, obtained by traditional Hartree–Fock calculations, by calculations with inclusion of correlation effects using the Møller–Plesset perturbation theory, and by DFT calculations; (2) determination of the potential functions of internal rotation in liquid anisole; and (3) quantitative characterization of intramolecular interactions in anisole molecule using the Natural Bond Orbitals (NBO) approach.

The *ab initio* quantum-chemical calculations were performed in the one-determinant Hartree–Fock (HF) approximation [19]. The correlation energy was included using the computational schemes of the second-order Møller–Plesset perturbation theory [19, 20]. The correlation correction was applied for all the orbitals: MP2(*f*). In DFT calculations [21], we used the B3LYP hybrid electron density functional modified in the GAUSSIAN programs [22, 23]. The potential function of internal rotation about the $C_{sp^2}$–O bond in the liquid phase was calculated using the self-consistent reactive field (SCRF) continual model [24–26]. The calculations were performed in the 6-31G(*d*) basis set with four petal *sd* functions [27]. The standard convergence criteria were used for the density matrix and energy gradient. All the calculations were performed in the range of torsion angles φ from 0° to 90° at a 15° step. The stationary points obtained in the MP2(f)/6-31G(*d*) and B3LYP/6-31G(*d*) approximations were refined and identified with full geometry optimization (including the torsion angle φ) and solution of vibrational problems. Computations were performed with the GAUSSIAN 98W software [28]. The population analysis for the wave functions obtained in the MP2(f)/6-31G(*d*) approximation was performed by the NBO method [29–31] using the NBO program, Version 3.1 (link 607, GAUSSIAN 98W) [32].

The total energies ($E_{tot}$, au) of the $C_6H_5OCH_3$ molecule, obtained by HF/6-31G(*d*), MP2(f)/6-31G(*d*), and B3LYP/6-31G(*d*) calculations for the φ range from 0° to 90° at a a 15° step, are listed in Table 1. In parentheses are the energies of particular conformers ($\Delta E$, kJ mol$^{-1}$) relative to the global minimum.

The HF/6-31G(*d*) calculations show that the global minimum of the potential energy function of internal rotation around the $C_{sp^2}$–O bond lies in the region of the planar conformation. However, a less deep (local) minimum is also observed in the region of the orthogonal form (Fig. 1, curve 1). The maximum is observed at φ ~60°. The barrier to transition of the molecule from the planar to orthogonal form (without correction for the zero vibration energy and with the accuracy determined by the 15° step) is 6.65 kJ mol$^{-1}$, and the barrier to transition from the orthogonal to planar form, 0.83 kJ mol$^{-1}$.

When the correlation energy [MP2(f)/6-31G(*d*) approximation] is taken into account, the shape of the potential function of internal rotation around the $C_{sp^2}$–O bond changes. Calculations show that the rotation barrier in $C_6H_5OCH_3$ is twofold, with the energy minimum in the region of the planar form and the maximum in the region of the orthogonal form (Fig. 1, curve *2*). The rotation barrier, without correction for the zero-point energy, is 9.48 kJ mol$^{-1}$. The molecular geometry, including φ, was fully optimized in the MP2(*f*)/6-31G(*d*) approximation, and the vibrational problems were solved at the stationary points. In the point of the total energy minimum (φ 0°), the matrix of second derivatives (Hesse matrix) has only positive eigenvalues, and in the point of the maximum (φ 90°) there is one negative eigenvalue (–45.56 cm$^{-1}$). The corrections for the zero vibration energy (taking into account the scaling factor of 0.9661 [33]) are 0.129984 (φ 0°) and 0.129339 hartree/particle (φ 90°). The rotation barrier corrected for the zero vibration energy is 7.78 kJ mol$^{-1}$.

The DFT calculations using the B3LYP three-parameter hybrid functional also show that the energy minimum of the potential function of internal rotation around the $C_{sp^2}$–O bond in the $C_6H_5OCH_3$ molecule lies in the region of the planar conformation, and the maximum, in the region of the orthogonal form (Fig. 1, curve *3*). The rotation barrier without correction for the zero-point energy is 12.63 kJ mol$^{-1}$. We have fully optimized the molecular geometry, including φ, and solved the vibrational problems in the stationary points. In the point of the total energy minimum (φ 0°), the Hesse matrix has only positive eigenvalues, and in the point of the maximum (φ 90°), one negative eigenvalue (–47.60 cm$^{-1}$). The corrections for the zero-point energy (scaling factor 0.9806 [33]) are 0.131037 (φ 0°) and 0.130302 hartree/particle (φ 90°). The rotation barrier corrected for the zero-point energy is 10.70 kJ mol$^{-1}$.

Thus, Hartree–Fock calculations of the anisole molecule reveal a fourfold barrier to rotation about the $C_{sp^2}$–O bond, but calculations taking into account the correlation energy show that the barrier is twofold.

**Table 1.** Total energy ($E_{tot}$, au) of the anisole molecule, obtained by HF/6-31G(*d*), MP2/6-31G(*d*), and B3LYP/6-31G(*d*) calculations for the range of the torsion angle φ from 0° to 90°[a]

| Method | φ, deg | | | | | | |
|---|---|---|---|---|---|---|---|
| | 0 | 15 | 30 | 45 | 60 | 75 | 90 |
| | | | | In vacuum | | | |
| HF/6-31G(*d*) | 344.5832616 (0.00) | 344.5829434 (0.84) | 344.582109 (3.03) | 344.581144 (5.56) | 344.5807327 (6.64) | 344.5809207 (6.15) | 344.5810447 (5.82) |
| MP2/6-31G(*d*) | 345.6831291 (0.00) | 345.6827475 (1.00) | 345.6817110 (3.72) | 345.6804153 (7.13) | 345.6796587 (9.11) | 345.6795371 (9.43) | 345.6795188 (9.48) |
| B3LYP/6-31G(*d*) | 346.7713725 (0.00) | 346.7709401 (0.96) | 346.7697279 (3.58.) | 346.7981216 (6.87) | 346.7670415 (8.78) | 346.7666722 (9.08) | 346.7666147 (9.14) |
| | | | | SCRF | | | |
| HF/6-31G(*d*) | 344.5835005 (0.00) | 344.5831781 (0.85) | 344.5823694 (2.97) | 344.5814074 (5.50) | 344.5810044 (6.55) | 344.5811976 (6.05) | 344.5813058 (5.76) |
| MP2/6-31G(*d*)// MP2/6-31G(*d*) | 345.6833588 (0.00) | 345.682999 (0.94) | 345.681959 (0.368) | 345.6806473 (7.12) | 345.6798974 (9.09) | 345.6797943 (9.36) | 345.6797704 (9.42) |

[a] The relative energies $\Delta E = E_{min} - E_{\varphi}$ (kJ mol$^{-1}$) are given in parentheses.

An appreciable difference between the barriers to rotation around the $C_{sp^2}$–O bond estimated by MP2 (7.78 kJ mol$^{-1}$) and B3LYP (10.70 kJ mol$^{-1}$) calculations is worth noting. This difference arises when the correction for the zero-point energy is taken into account. The B3LYP approximation overestimates the stability of the planar form compared to the MP2 method.

According to electron diffraction data [1, 2], in the gas phase the COC bond angle is 120.9(6)°, and the bond lengths, $l$($C_{sp^2}$–O) 1.357(6) and $l$($C_{sp^3}$–O) 1.423(7) Å. Analysis of the microwave spectrum gives the C–O bond length of 1.399 Å and COC bond angle of 113.8° [1, 3]. The optimized bond angles and bond lengths in the $C_6H_5OCH_3$ molecule at fixed φ values in the range 0°–90° are listed in Table 2. In the planar conformation, the COC bond angle is estimated at ~120° (HF), 117° (MP2), and 118° (B3LYP); the $C_{sp^2}$–O bond length, at 1.35 (HF), 1.37 (MP2), and 1.37 Å (B3LYP); and the $C_{sp^3}$–O bond length, at 1.40 (HF), 1.42 (MP2), and 1.42 Å (B3LYP).

The first Koopmans ionization potentials ($^1I_K$) obtained by HF and MP2 calculations virtually coincide. Therefore, we give only the $^1I_K$ values obtained by MP2 calculations (eV; the φ values are given in parentheses): 8.32 (0°), 8.34 (15°), 8.39 (30°), 8.49 (45°), 8.62 (60°), 8.72 (75°), and 8.75 (90°). The experimental values of the first vertical ionization potential (photoelectron spectroscopy) are 8.42 [4] and 8.46 eV [5]. The $^1I_K$ values are sensitive to molecular conformation and grow in going from the planar to orthogonal form. The DFT potentials involve artificially overestimated one-electron energies, and, therefore, DFT calculations give appreciably underestimated ionization potentials [34]. The dipole moment ($\mu_D$) of the $C_6H_5OCH_3$ molecule (D) depending on the conformation (φ, in parentheses) is as follows: 1.35 (0°), 1.36 (15°), 1.37 (30°), 1.39 (45°), 1.41 (60°), 1.45 (75°), and 1.47 (90°) by the MP2 method and 1.31 (0°), 1.31 (15°), 1.30 (30°), 1.29 (45°), 1.29 (60°), 1.31 (75°), and 1.32 (90°) by the B3LYP method. The experimental values of $\mu_D$ range from 0.8 to 1.34 D [35]. In particular, the $\mu_D$ of anisole is 1.23 D

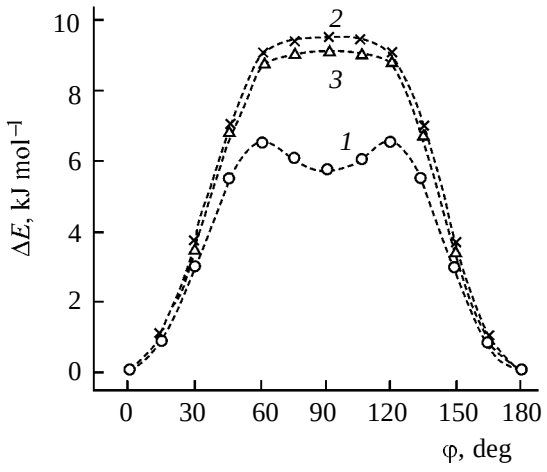


**Fig. 1.** Potential functions of internal rotation around the $C_{sp^2}$–O bond in the anisole molecule, obtained by (*1*) HF/6-31G(*d*), (*2*) MP2(*f*)/6-31G(*d*), and (*3*) B3LYP/6-31G(*d*) calculations.

**Table 2.** Optimized bond lengths (Å) and bond angles (deg) in the anisole molecule

| Parameter | Method | φ, deg | | | | | | |
|---|---|---|---|---|---|---|---|---|
| | | 0 | 15 | 30 | 45 | 60 | 75 | 90 |
| | | In vacuum | | | | | | |
| $l(C_{sp^2}–O)$ | HF | 1.350 | 1.351 | 1.353 | 1.357 | 1.361 | 1.363 | 1.363 |
| | DFT | 1.367 | 1.368 | 1.370 | 1.374 | 1.378 | 1.381 | 1.382 |
| | MP2 | 1.371 | 1.371 | 1.373 | 1.377 | 1.382 | 1.384 | 1.385 |
| $l(C_{sp^3}–O)$ | HF | 1.398 | 1.399 | 1.401 | 1.403 | 1.404 | 1.405 | 1.405 |
| | DFT | 1.417 | 1.418 | 1.421 | 1.423 | 1.424 | 1.424 | 1.425 |
| | MP2 | 1.422 | 1.423 | 1.425 | 1.427 | 1.428 | 1.429 | 1.429 |
| ∠COC | HF | 119.76 | 119.61 | 119.14 | 118.34 | 117.16 | 115.98 | 115.49 |
| | DFT | 118.31 | 118.13 | 117.75 | 117.08 | 116.05 | 114.85 | 114.32 |
| | MP2 | 116.79 | 116.62 | 116.12 | 115.24 | 113.88 | 112.51 | 111.94 |
| ∠CCO | HF | 124.54 | 124.32 | 123.70 | 122.91 | 121.93 | 120.75 | 119.88 |
| | DFT | 124.58 | 124.38 | 123.82 | 123.08 | 122.04 | 120.73 | 119.73 |
| | MP2 | 124.86 | 124.60 | 123.93 | 123.04 | 121.89 | 120.58 | 119.68 |
| | | In neat liquid | | | | | | |
| $l(C_{sp^2}–O)$ | HF | 1.349 | 1.350 | 1.353 | 1.357 | 1.361 | 1.363 | 1.363 |
| $l(C_{sp^3}–O)$ | HF | 1.399 | 1.400 | 1.402 | 1.404 | 1.405 | 1.405 | 1.406 |
| ∠COC | HF | 119.76 | 119.60 | 119.12 | 118.30 | 117.11 | 115.92 | 115.43 |
| ∠CCO | HF | 124.55 | 124.33 | 123.71 | 122.91 | 121.93 | 120.75 | 119.88 |

in benzene, 1.24 D in $CCl_4$ (second Debye method) [7], and 1.10 D in neat liquid (Onsager method) [36].

In the SCRF model, a solvent is described as a polarizable dielectric continuum characterized by the static dielectric constant ε. Anisole does not belong to standard solvents included in the GAUSSIAN 98W program; we took for anisole the value ε of 4.33 [37]. The cavity volume was calculated according to [38] using the Tight parameter. To take into account the effect of the medium on the relaxation of the geometric parameters, we optimized the geometry in the HF/6-31G(*d*) approximation. As in the case of standard (without inclusion of medium effects) HF/6-31G(*d*) calculations, two minima are revealed for the potential function of internal rotation about the $C_{sp^2}–O$ bond: a deeper minimum in the region of the planar conformation and a less deep minimum in the region of the orthogonal form. The rotation barrier obtained for the liquid and isolated molecule in a vacuum differ insignificantly (Table 1). The geometries also differ only slightly (Table 2). The geometric parameters could not be optimized within the framework of the SCRF model in Møller–Plesset calculations; therefore, in the MP2(f)/6-31G(*d*) calculations for liquid anisole we used the geometry obtained in the same approximation for the gas phase: $MP2(f)/6\text{-}31G(d)_{liq}//MP2(f)/6\text{-}31G(d)_{vac}$. The profile of the potential function of internal rotation about the $C_{sp^2}–O$ bond and the height of the rotation barrier in liquid anisole, calculated with inclusion of correlation effects, only slightly differ from those obtained for the isolated molecule in a vacuum (Table 1).

The NBO analysis involves a set of methods based on successive transformation of the initial nonorthogonal set of canonical molecular orbitals into natural atomic orbitals (NAO), natural hybrid orbitals (NHO), natural bond orbitals (NBO), and natural localized molecular orbitals (NLMO) [29–31]. This allows interpretation of the quantum-chemical results in terms of the classical Lewis concepts of molecular structure. The hybridization state ($s_n$), energy ($E_n$), and population ($P_n$) of the oxygen lone electron pairs and the energies of their interaction with antibonding π* orbitals of the aromatic moiety ($E_{n,\pi}$) in conformations characterized by the torsion angles φ from 0° to 90° (15° step) are listed in Table 3. According to the NBO approach, the two lone electron pairs at the O atom are essentially different. One of the pairs (*n*1) is a hybrid orbital with the contribution of the *s* constituent varying from ~38 to ~45% depending on φ. The second lone electron pair (*n*2) is a virtually pure *p* orbital. As the anisole molecule exists in the planar conformation, the contribution of the s constituent to *n*1 can be estimated at ~41%. The *n*1 orbital lies considerably lower on the energy scale than *n*2, and its population is higher than that of *n*2. As φ is increased from 0° to

**Table 3.** Degree of hybridization ($s_n$, %), energy ($E_n$, eV), and population ($P_n$, e) of the oxygen lone electron pairs, energy of their interaction with the antibonding π* orbitals of the aromatic ring ($E_{n,\pi}$, kJ mol$^{-1}$), and natural charges ($q$, e) on atoms

| Parameter | φ, deg | | | | | | |
|---|---|---|---|---|---|---|---|
| | 0 | 15 | 30 | 45 | 60 | 75 | 90 |
| $s_{n1}$ | 40.9 | 40.7 | 40.2 | 39.5 | 38.5 | 38.8 | 45.0 |
| $s_{n2}$ | 0.0 | 0.3 | 1.4 | 3.1 | 5.3 | 5.9 | 0.0 |
| $-E_{n1}$ | 21.42 | 21.37 | 21.22 | 20.99 | 20.71 | 20.72 | 21.89 |
| $-E_{n2}$ | 13.03 | 13.10 | 13.31 | 13.66 | 14.13 | 14.28 | 13.17 |
| $P_{n1}$ | 1.94076 | 1.94050 | 1.93958 | 1.93745 | 1.93332 | 1.92778 | 1.92321 |
| $P_{n2}$ | 1.83212 | 1.83583 | 1.84672 | 1.86419 | 1.88456 | 1.90081 | 1.90926 |
| $E_{n1,\pi}$ | 0.0 | 0.0 | 0.0 | 4.7 | 8.8 | 17.3 | 30.1 |
| $E_{n2,\pi}$ | 146.9 | 139.5 | 118.9 | 88.4 | 54.4 | 25.9 | 0.0 |
| $-q$(O) | 0.5306 | 0.5329 | 0.5394 | 0.5489 | 0.5581 | 0.5637 | 0.5656 |
| $q$(C$_i$) | 0.3061 | 0.3053 | 0.3030 | 0.2990 | 0.2944 | 0.2909 | 0.2896 |
| $-\Sigma q$(C$_o$)/2 | 0.2880 | 0.2866 | 0.2826 | 0.2768 | 0.2715 | 0.2686 | 0.2675 |
| $q$(H$_o$)/2 | 0.2427 | 0.2428 | 0.2428 | 0.2430 | 0.2435 | 0.2445 | 0.2449 |
| $-\Sigma q$(C$_m$)/2 | 0.2298 | 0.2299 | 0.2301 | 0.2306 | 0.2310 | 0.2318 | 0.2321 |
| $\Sigma q$(H$_m$)/2 | 0.2361 | 0.2362 | 0.2363 | 0.2366 | 0.2369 | 0.2371 | 0.2372 |
| $-q$(C$_p$) | 0.2515 | 0.2509 | 0.2493 | 0.2466 | 0.2435 | 0.2412 | 0.2403 |
| $q$(H$_p$) | 0.2358 | 0.2358 | 0.2359 | 0.2362 | 0.2365 | 0.2367 | 0.2368 |
| $-q$(C$_{Me}$) | 0.3095 | 0.3090 | 0.3072 | 0.3037 | 0.2990 | 0.2969 | 0.2965 |
| $q$(H$_{Me}$)/3 | 0.2092 | 0.2089 | 0.2081 | 0.2065 | 0.2047 | 0.2039 | 0.2037 |

90°, the population of $n1$ at the O atom decreases by ~0.018 e, and that of $n2$ increases by ~0.077 e. The increase in the population of the $n2$ orbital, which is a virtually pure $p$ orbital, in going from the planar to orthogonal conformation is due to distortion of the coplanarity leading to less pronounced delocalization of this orbital to the aromatic ring and its more pronounced localization on the heteroatom. However, the population of the hybrid lone electron pair $n1$ is also sensitive to the conformation, probably owing to the fairly high contribution of the $p$ constituent. As φ is increased, its population decreases. The parameters $E_{n,\pi}$ quantitatively characterize the donor–acceptor interactions of $n1$ and $n2$ with the antibonding π* orbitals of the aromatic ring. Figure 2 shows how $E_{n1,\pi}$ and $E_{n2,\pi}$ in anisole vary with the torsion angle φ. At zero and low φ, the hybrid lone electron pair $n1$ of the O atom virtually does not interact with the π* orbitals of the ring. However, in nonplanar conformations (starting from φ ~45°), the resonance interaction of $n1$ with the π* orbitals of the aromatic ring becomes noticeable, reaching a maximum (~30 kJ mol$^{-1}$) in the orthogonal form. The $n2$ pair, which is a virtually pure p orbital, interacts most efficiently with the antibonding π* orbitals of the aromatic ring in the planar conformation ($E_{n2,\pi}$ ~147 kJ mol$^{-1}$). As the torsion angle φ is increased, the interaction of $n2$ with π* drastically weakens, and in the orthogonal conformation there is virtually no resonance interaction of $n2$ with the ring. Thus, our results show that, in the orthogonal conformation, the O atom partially preserves the capability for resonance interaction with the aromatic ring owing to participation of the hybrid lone electron pair $n1$ in the $n,\pi$ conjugation.

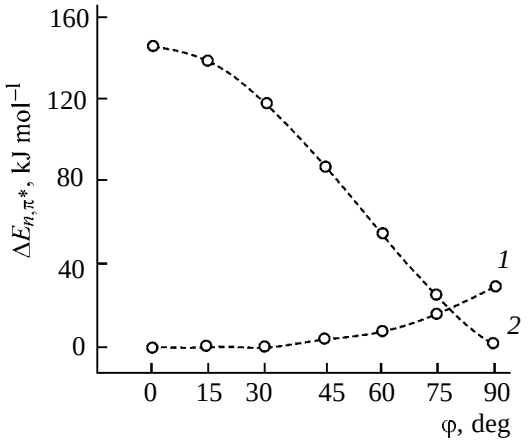


**Fig. 2.** Energy of interaction of oxygen lone electron pairs with antibonding π* orbitals of the aromatic ring as a function of the torsion angle φ: (*1*) $n1$ and (*2*) $n2$.

**Table 4.** Difference between the atomic charges ($\Delta q$, e) in the aromatic ring of anisole and in unsubstituted benzene, $\Delta q = q(C_6H_5OCH_3) - q(C_6H_6)$

| Parameter | φ, deg | | | | | | |
|---|---|---|---|---|---|---|---|
| | 0 | 15 | 30 | 45 | 60 | 75 | 90 |
| $q(C_i)$ | 0.5411 | 0.5403 | 0.5380 | 0.5340 | 0.5294 | 0.5259 | 0.5246 |
| $-\Sigma q(C_o)/2$ | 0.0530 | 0.0516 | 0.0476 | 0.0418 | 0.0365 | 0.0336 | 0.0325 |
| $\Sigma q(H_o)/2$ | 0.0077 | 0.0078 | 0.0078 | 0.0080 | 0.0085 | 0.0095 | 0.0099 |
| $\Sigma q(C_m)/2$ | 0.0053 | 0.0051 | 0.0049 | 0.0044 | 0.0040 | 0.0032 | 0.0029 |
| $\Sigma q(H_m)/2$ | 0.0011 | 0.0012 | 0.0013 | 0.0016 | 0.0019 | 0.0021 | 0.0022 |
| $-q(C_p)$ | 0.0165 | 0.0159 | 0.0143 | 0.0116 | 0.0085 | 0.0062 | 0.0053 |
| $q(H_p)$ | 0.0008 | 0.0008 | 0.0009 | 0.0012 | 0.0015 | 0.0017 | 0.0018 |

The natural charges obtained from the natural populations improve the description of the electron density distribution in the molecule as compared to the traditional Mulliken analysis [39]. The natural atomic charges in the anisole molecule are listed in Table 3. From these values, we can determine the direction of bond polarization. Owing to the higher electronegativity of O compared to the *ipso*-C atom of the ring, the $C_i \rightarrow O$ bond is polarized toward O; the $C_i$ atom is electron-deficient, and the O atom, electron-excessive. Irrespective of the conformation, the $C_i \rightarrow C_o$ and $C_m \rightarrow C_o$ bonds are polarized toward the *o*-C atoms, and the $C_m \rightarrow C_p$ bonds, toward the *p*-C atom. The $O \leftarrow C_{Me}$ bond is polarized toward O, and the $C_{Me}$–H bonds, toward $C_{Me}$.

It is convenient to consider the effect of the $OCH_3$ group on the electron density distribution in the aromatic fragment by examining the differences between the atomic charges in anisole and unsubstituted benzene: $\Delta q = q$(anisole) – $q$(benzene). The MP2(*f*)/6-31G(*d*) calculation of the unsubstituted benzene molecule, followed by NBO analysis of the wave function, gives the natural atomic charges of –0.2350 e for each carbon atom and 0.2350 e for each hydrogen atom. The $\Delta q$ values are given in Table 4 in parentheses. The higher negative value of $\Delta q$ (or lower positive value of $\Delta q$) corresponds to the higher electronic charge on the given atom as compared to the corresponding atom (C or H) in unsubstituted benzene. The $\Delta q(C_i)$ values (~0.52–0.54 e) reveal a strong acceptor effect of the $OCH_3$ group on the $C_i$ atom. The interaction of the $n2$ oxygen lone electron pair with the π* orbitals of the ring is the most pronounced in the planar conformation. Therefore, in the planar conformation the $\Delta q$ values for the $C_o$ (–0.0784 and –0.0275 e) and $C_p$ (–0.0165 e) atoms are the most negative. In the orthogonal conformation, the weak electron-donor effect on the *o*- and *p*-positions of the ring [$\Delta q(C_o) \sim -0.03$ e and $\Delta q(C_p) \sim -0.005$ e] is preserved. As shown above, this is due to the resonance interaction of the hybrid lone electron pair $n1$ with the antibonding π* orbitals of the ring. The $OCH_3$ group has an acceptor effect on the $C_m$ atoms and hydrogen atoms of the aromatic moiety. A $^{13}C$ NMR study of $C_6H_5OAlk$ (Alk = Me, Et, Pr-*i*, or Bu-*t*) [40] showed that the molecular conformation varied depending on the steric demands of alkyl substituents. In the $C_6H_5OBu$-*t* molecule existing in the orthogonal or close-to-orthogonal form [5], the *p*-C atoms ($\delta_{C_p}$ 122.88 ppm [40]) are more shielded than in unsubstituted benzene ($\delta_C$ 128.5 ppm [41]). The strong shielding of the $^{13}C_p$ nuclei in the $C_6H_5OBu$-*t* molecule is an experimental evidence of the capability of the O atom to preserve the resonance interaction with the aromatic ring in nonpolar (close-to-orthogonal) conformations.

## ACKNOWLEDGMENTS

The study was financially supported by the Ukrainian State Foundation for Basic Research (project no. F-7/334).

## REFERENCES

1. Naumov, V.A. and Kataeva, O.N., *Molekulyarnoe stroenie organicheskikh soedinenii kisloroda i sery v gazovoi faze* (Molecular Structure of Organic Compounds of Oxygen and Sulfur in the Gas Phase), Moscow: Nauka, 1990.
2. Seip, H.M. and Seip, R., *Acta Chem. Scand.*, 1973, vol. 27, no. 10, p. 4024.
3. Onda, M., Toda, A., Mori, S., and Yamaguchi, I., *J. Mol. Struct.*, 1986, vol. 144, no. 1/2, p. 47.
4. Maier, J.P. and Turner, D.W., *J. Chem. Soc., Faraday Trans. 2*, 1973, vol. 69, no. 4, p. 521.

5. Dewar, P.S., Ernstbrunner, E., Gilmore, J.R., Godfrey, M., and Mellor, J.M., *Tetrahedron*, 1974, vol. 30, no. 15, p. 2455.
6. Le Fevre, R.J.W., Radford, D.V., and Sullivan, E.P.A., *Aust. J. Chem.*, 1967, vol. 20, no. 4, p. 623.
7. Aroney, M.J., Le Fevre, R.J.W., Pierens, R.K., and The, M.G.N., *J. Chem. Soc. B*, 1969, no. 6, p. 666.
8. Schaefer, T. and Sebastian, R., *Can. J. Chem.*, 1989, vol. 67, no. 7, p. 1148.
9. Allen, J. and Fewster, S., *Internal Rotation of Molecules*, Orville-Thomas, W.J., Ed., London: Wiley, 1974. Translated under the title *Vnutrennee vrashchenie molekul*, Moscow: Mir, 1977, p. 211.
10. Frige, H. and Klessinger, M., *Chem. Ber.*, 1979, vol. 112, no. 5, p. 1614.
11. Konshin, H. and Tylli, H., *Chem. Phys. Lett.*, 1984, vol. 108, no. 2, p. 191.
12. Konschin, H. and Lindblad, M., *J. Mol. Struct.*, 1983, vol. 104, nos. 1–2, p. 37.
13. Owen, N.L. and Hester, R.E., *Spectrochim. Acta, Part A*, 1969, vol. 25, no. 2, p. 343.
14. Tylli, H. and Konschin, H., *J. Mol. Struct.*, 1977, vol. 42, no. 1, p. 7.
15. Konschin, H., Tylli, H., and Grundfelt-Forsius, C., *J. Mol. Struct.*, 1981, vol. 77, nos. 1–2, p. 51.
16. Vincent, M.A. and Hillier, I.H., *Chem. Phys.*, 1990, vol. 140, no. 1, p. 35.
17. Spellmeyer, D.C., Grootenhuis, P.D.J., Miller, M.D., Kuyper, L.F., and Kollman, P.A., *J. Phys. Chem.*, 1990, vol. 94, no. 11, p. 4483.
18. Nicholas, J.B. and Hay, B.P., *J. Phys. Chem.*, 1999, vol. 103, no. 48, p. 9815.
19. Hehre, W.J., Radom, L., Schleyer, P.v.R., and Pople, J.A., *Ab initio Molecular Orbital Theory*, New York: Wiley, 1986.
20. Møller, Ch. and Plesset, M.S., *Phys. Rev.*, 1934, vol. 46, no. 4, p. 618.
21. Parr, R.G. and Yang, W., *Density Functional Theory of Atoms and Molecules*, New York: Oxford Univ. Press, 1989.
22. Becke, A.D., *J. Chem. Phys.*, 1993, vol. 98, no. 7, p. 5648.
23. Stephens, P.J., Delvin, C.F., Chabalowski, C.F., and Frisch, M.J., *J. Phys. Chem.*, 1994, vol. 98, no. 45, p. 11623.
24. Tapia, O. and Goskinski, O., *Mol. Phys.*, 1975, vol. 29, no. 6, p. 1653.
25. Wong, M.W., Frisch, M.J., and Wiberg, K.B., *J. Am. Chem. Soc.*, 1991, vol. 113, no. 13, p. 4776.
26. Abronin, I.A., Burshtein, K.Ya., and Zhidomirov, G.M., *Zh. Strukt. Khim.*, 1980, vol. 21, no. 2, p. 145.
27. Hariharan, P.C. and Pople, J.A., *Theor. Chim. Acta*, 1973, vol. 28, no. 3, p. 213.
28. Frisch, M.J., Trucks, G.W., Schlegel, H.B., Scuseria, G.E., Robb, M.A., Cheeseman, J.R., Zakrzewski, V.G., Montgomery, J.A., Stratmann, R.E., Burant, J.C., Dapprich, S., Barone, V., Cossi, M., Cammi, R., Mennucci, B., Adamo, C., Clifford, S., Ocherski, J., Petersson, G.A., Ayala, P.Y., Cui, Q., Morokuma, K., Malick, D.K., Rabuck, A.D., Raghavachari, K., Foresman, J.B., Cioslowski, J., Ortiz, J.V., Stefanov, B.B., Liu, G., Liashenko, A., Piskorz, P., Komaromi, I., Gomperts, R., Martin, R.L., Fox, D.J., Keith, T.A., Al-Laham, M.A., Peng, C.Y., Nanayakara, A., Gonzalez, C., Challacombe, M., Gill, P.M.W., Johnson, B.G., Chen, W., Wong, M.W., Andres, J.L., Head-Gordon, M., Replogle, E.S., and Pople, J.A., *GAUSSIAN 98W*, Rev. A.7, Pittsburgh: Gaussian, 1998.
29. Weinhold, F. and Carpenter, J.E., *The Structure of Small Molecules and Ions*, Naaman R. and Vager, Z., Eds., New York: Plenum, 1988, p. 227.
30. Reed, A.E., Curtiss, L.A., and Weinhold, F., *Chem. Rev.*, 1988, vol. 88, no. 6, p. 899.
31. Nemukhin, A.V. and Veinkhol'd, F., *Ross. Khim. Zh.*, 1994, vol. 38, no. 6, p. 5.
32. Glendening, E.D., Reed, A.E., Carpenter, J.E., and Weinhold, F., *GAUSSIAN 98W*, Rev. A.7, NBO Ver. 3.1, Pittsburgh: Gaussian, 1998.
33. Scott, A.P. and Radom, L., *J. Phys. Chem.*, 1996, vol. 100, no. 41, p. 16502.
34. van Leenuwen, R. and Baerends, E.J., *Phys. Rev. A*, 1994, vol. 49, no. 4, p. 2421.
35. Osipov, O.A., Minkin, V.I., and Garnovskii, A.D., *Spravochnik po dipol'nym momentam* (Handbook on Dipole Moments), Moscow: Vysshaya Shkola, 1971.
36. Borovikov, Yu.Ya. and Topchii, V.A., *Teor. Eksp. Khim.*, 1975, vol. 11, no. 1, p. 108.
37. Gordon, A.J. and Ford, R.A., *The Chemist's Companion. A Handbook of Practical Data, Techniques, and References*, New York: Wiley, 1972.
38. Frisch, A. and Frisch, M.J., *GAUSSIAN 98 User's Reference*, Pittsburgh: Gaussian, 1999.
39. Reed, A.E., Weinstock, R.B., and Weinhold, F., *J. Chem. Phys.*, 1985, vol. 83, no. 2, p. 735.
40. Bzhezovskii, V.M., Kalabin, G.A., Aliev, I.A., Trofimov, B.A., Shakhgel'diev, M.A., and Kuliev, A.M., *Izv. Akad. Nauk SSSR, Ser. Khim.*, 1976, no. 9, p. 1999.
41. Breitmaier, E. and Voelter, W., *Carbon-13 NMR Spectroscopy*, Weinheim: VCH, 1987.